$\mathbf{O(N^2 \log N)}$ NATIVE FAN-BEAM TOMOGRAPHIC RECONSTRUCTION

Shu Xiao, Yoram Bresler, and David C. Munson, Jr.

Department of Electrical and Computer Engineering and
Coordinated Science Laboratory
University of Illinois at Urbana–Champaign
1308 West Main Street
Urbana, IL 61801, USA

ABSTRACT

We present a new fast backprojection algorithm for CT fan-beam reconstruction. The new algorithm operates directly on fan-beam data without prior rebinning to parallel-beam projections. The algorithm reduces the computational complexity from $O(N^3)$ for the traditional fan-beam algorithm to $O(N^2 \log N)$. Simulations demonstrate speedups of greater than 50-fold for a 512×512 image, with no perceivable degradation in accuracy. The algorithm also applies to multi-slice helical 3D reconstruction, and extends to 3D cone-beam reconstruction.

1. INTRODUCTION

The dominant mode of acquisition in axial CT is the fan-beam geometry [1–3]. Although originally a 2D method, fan-beam reconstruction is also the key component in state-of-the-art methods for helical and multi-slice helical 3D (volumetric) reconstruction (see [2] and the references therein). As in parallel-beam tomography, the preferred procedure for image reconstruction from fan-beam data is of the filtered-backprojection (FBP) type. Compared to parallel-beam CT, this procedure involves some additional weighting before filtering and in the backprojection itself, and is known as fan-beam FBP (FB-FBP). The computation cost of FB-FBP is dominated by the (fan-beam) backprojection, which has computational complexity $O(N^3)$ for a $N \times N$-pixel image. This unfavorable scaling with resolution N, and the high data rates in 3D, and in particular in real-time applications (e.g., cardiac or interventional imaging), motivate the study of fast algorithms for fan-beam reconstruction.

Significant progress has been made recently in fast algorithms for the parallel-beam geometry [4]. These algorithm have a computational cost of $O(N^2 \log N)$ instead of $O(N^3)$ as for conventional algorithms, and they offer speedups on the order of a 100-fold for practical image sizes. Other fast algorithms for the parallel-beam geometry include FFT methods based on the projection-slice theorem [3], and the interrelated methods of [5–8], and their precursors (see [4] for a survey and comparison).

All fast parallel-beam algorithms can be applied to fan-beam tomography after rebinning the fan-beam data [1–3]. The rebinning procedure rearranges and interpolates fan-beam-generated projections to create a new set of parallel-beam projections. This requires a two-dimensional interpolation of ray sums in both angular and radial directions. Higher-order interpolation can be used for better image quality at the expense of more computations. The drawbacks of rebinning include possible artifacts and added computation. This limits the speedup obtained by the combination of rebinning and fast parallel-beam algorithms, as compared to conventional fan-beam reconstruction.

Only limited work has been reported on fast "native" fan-beam algorithms, which operate directly on fan-beam data, without prior rebinning to parallel-beam. Initially developed for parallel-beam data, Nilsson's "link-based" fast backprojection algorithm was approximately extended to fan-beam geometry [5–7]. Owing to the approximation involved in this extension, at best only a modest speedup can be obtained without objectionable image degradation. In fact, [7] concluded that the only approach that provided adequate accuracy involved rebinning first to parallel-beam data. We are not aware of effective fast algorithms for *native* fan-beam backprojection.

Here, we propose a novel, fast native fan-beam reconstruction algorithm without a rebinning process. Like its parallel-beam counterpart [4], our fan-beam algorithm requires $O(N^2 \log N)$ time for reconstruction. It provides significant speedup over conventional exact fan-beam backprojection for typical image sizes, without perceivable degradation in image quality.

2. FAN-BEAM IMAGING GEOMETRIES AND CONVENTIONAL RECONSTRUCTION

The two most common fan-beam sampling geometries involve colinear equispaced, or equiangularly spaced detectors [1] Other geometries are also of interest, including the extension to 3D helical fan-beam scan. In all cases, the reconstruction consists of a step of weighting and filtering, followed by weighted fan-beam backprojection. The computational cost of the latter dominates conventional reconstruction algorithms, and is therefore the target of our fast algorithm. For the sake of brevity, we discuss only one representative geometry.

The colinear equispaced fan-beam geometry, where the detectors are evenly spaced on a straight line is illustrated in Fig. 1 The source S of divergent rays travels on a circular trajectory of radius D centered at the origin O, with the detector line rotating with it. The source position is indicated by the *source angle* θ. The detector line (the t axis) is assumed, without loss of generality, to pass through the center of rotation O of the source, and to be perpendicular to the source-to-center line $\overline{SO}$. Otherwise, simple linear

This work was supported by DARPA grant F49620-98-1-0498 administered by AFSOR, DARPA grant DAAG55-98-1-0039 administered by ARO, and NSF grant CCR-99-72980.

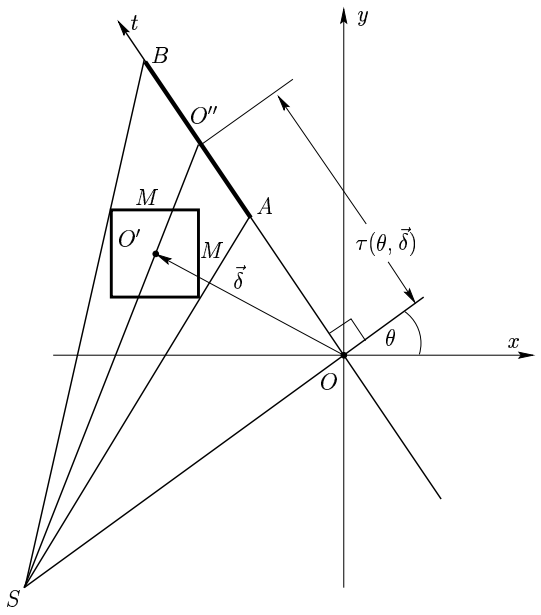

Fig. 1. Colinear equispaced fan-beam projection geometry for an $M \times M$ subimage

coordinate scaling will convert the actual detector positions to the uniform spacing on the new detector line.

Let $\vec{r} = [x, y]^T$ denote position in the image, and let $\tau(\theta, \vec{r})$ denote the t position of the intersection with the t-axis of the source ray passing through point $\vec{r}$ (see Fig. 1, where $\tau(\theta, \vec{\delta})$ is shown). The fan-beam projection $(\mathcal{P}f)(\theta, t)$ of the object f at source angle θ and detector position t is the line integral along the source ray parametrized by (θ, t). Projections are acquired at P discrete source angles $\theta_p = p\Delta\theta, p = 0, \ldots P-1$ with uniform spacing $\Delta\theta = \theta_{max}/P$. We call $(\mathcal{P}f)(\theta_p, \cdot)$ (for all values of t) a projection at source angle θ_p. The maximum source angle θ_{max} is equal to 2π in the case of a full scan, but can take other values in the case of short scan or over-scan [1].

Native (direct) inversion of fan-beam data can be formulated as a weighted filtered backprojection [1, 3]. First, the fan-beam projections are individually weighted and ramp-filtered producing the modified fan-beam projections $g(p, t)$, corresponding to source angles θ_p. For the sake of conciseness and generality, we will call the function $g(p, \cdot)$ itself (for fixed p) a fan-beam projection (at angle θ_p). The image is then reconstructed by the conventional discrete-angle backprojection

$$f(\vec{r}) = \sum_{p=0}^{P-1} W(p\Delta\theta, \vec{r}) g[p, \tau(p\Delta\theta, \vec{r})]\Delta\theta\,, \qquad (1)$$

where $W(\theta, \vec{r})$ is an appropriate weight function. In practice, $g(p, t)$ is also sampled in t, because of the use of discrete detectors. This requires interpolation of g in t to implement the backprojection, because $\tau(p\Delta\theta, \vec{r})$ does not usually correspond to an available sample position.

Because the computational cost of weighting and ramp filtering is only $O(N^2 \log N)$ when the convolution is performed using FFTs, the $O(N^3)$ cost of backprojection dominates the cost of conventional fan-beam reconstruction.

3. FAST NATIVE HIERARCHICAL ALGORITHM

The fast fan-beam backprojection algorithm is inspired by the fast hierarchical backprojection algorithm (FHBP) for parallel-beam tomography [4]. The basic idea in the parallel-beam FHBP algorithm is to partition a large $N \times N$ image f into four subimages $f_i, i = 1, \ldots 4$, each of size $N/2 \times N/2$. Two properties of the Radon transform are used in the derivation of the algorithm: (i) the bow-tie property [3] says that for a half-sized image centered at the origin, the spectral support of the projections with respect to the angular variable is also decreased by half. This implies that a centered half-sized image can be reconstructed from half the number of projections; (ii) the shift property says that the parallel projections of a shifted image correspond to shifted parallel projections of the original image.

Suppose now that P filtered projections are available to reconstruct the entire image f. To reconstruct one of the subimages f_i, the P projections are first truncated to the support of the projection of the subimage, then shifted to correspond to a centered version of the subimage, and finally decimated to $P/2$ projections with respect to the angular direction. The centered version of subimage f_i is then reconstructed from these new $P/2$ projections, and the subimage shifted back to its correct location. This is performed for each of the four subimages, which together provide a reconstruction of the entire image f.

A total of $4c(P/2)(N/2)^2 = cPN^2/2$ operations is necessary to reconstruct four subimages. This reduces the original reconstruction cost by half. Applying the decomposition recursively where the image size is decreased by half at each step, the total computational cost can be reduced to $O(N^2 \log N)$. The FHBP algorithm has been fully explained in [4].

Here we construct such a hierarchical algorithm to process fan-beam projections directly, without first rebinning to parallel beam data. We implement the same type of hierarchical structure, to reconstruct half-sized images from half the number of fan projections. An immediate difficulty that arises when trying to apply the ideas of the parallel beam FHBP to the fan-beam scenario, is that the shift property no longer applies. That is, the fan-beam projections of a shifted image, do not correspond to shifted projections of the original subimage. Because the parallel beam FHBP uses this property, the approach must be modified for the fan-beam scenario.

Consider the backprojection operation for a subimage $f'(\vec{r})$ of f, shown in Fig. 1. Let $\mathcal{K}_M[\vec{\delta}]$ be an image truncation operator such that $f' = \mathcal{K}_M[\vec{\delta}]f$ is a subimage of f of size $M \times M$ centered at $O' = \vec{\delta} \in \mathbb{R}^2$. The backprojection onto subimage f' using Q projections at source angles $p\Delta\theta,\ p = 0 \ldots Q-1$ follows directly from (1) and is given by $f'(\vec{r}) = \mathcal{B}_{M,Q}[\vec{\delta}]g(\vec{r})$ where $\mathcal{B}_{M,Q}[\vec{\delta}]$ is the associated backprojection operator. Thus, in particular, $f = \mathcal{B}_{N,P}[\vec{0}]g$.

Because of the locality of the backprojection, only part of the projection $g(p, \cdot)$ contributes to the backprojection onto f'. We denote this part by $\hat{\mathcal{K}}_M[\vec{\delta}]g$, where $\hat{\mathcal{K}}_M[\vec{\delta}]$ is the operator that, for each θ_p, truncates $g(p, \cdot)$ in t to the support $\overline{AB}$ of the projection of the support of the subimage $f' = \mathcal{K}_M[\vec{\delta}]f$ (see Fig. 1). The truncation intervals determining $\hat{\mathcal{K}}_M[\vec{\delta}]$ can be precomputed for all angles θ_p, and subimage sizes M and locations $\vec{\delta}$ of interest.

It follows from the localization of backprojection that if $f =$

$\mathcal{B}_{N,P}[\vec{0}]g$ then

$$f' = \mathcal{K}_M[\vec{\delta}]f = \mathcal{B}_{M,P}[\vec{\delta}]\hat{\mathcal{K}}_M[\vec{\delta}]g, \tag{2}$$

that is, the backprojection onto f' can be obtained by a backprojection of size (M, P) of the appropriately truncated projections. Consider now a partition of the image f into 4 nonoverlapping subimages, each of size $(N/2) \times (N/2)$,

$$f = \sum_{j=1}^{4} \mathcal{K}_{N/2}[\vec{\delta}_j]f, \tag{3}$$

where $\vec{\delta}_j, j = 1, \ldots 4$ are the centers of the subimages. Applying (2), we obtain the following exact decomposition for the backprojection, into backprojections onto the subimages.

$$f = \mathcal{B}_{N,P}[\vec{0}]g = \sum_{j=1}^{4} \mathcal{B}_{N/2,P}[\vec{\delta}_j]\hat{\mathcal{K}}_{N/2}[\vec{\delta}_j]g\,. \tag{4}$$

By itself, this decomposition does not provide a speedup compared to single-step backprojection $\mathcal{B}_{N,P}$. Indeed, while the computational cost $c(N/2)^2P$ of single subimage backprojection $\mathcal{B}_{M,P}$ is 4 times smaller than for the single-step $\mathcal{B}_{N,P}$ for the full image, the total cost for the required 4 such subimage backprojections remains the same (possibly with some small additional overhead for bookkeeping).

The fast algorithm is based on reconstruction of a subimage $f' = \mathcal{K}_M[\vec{\delta}]f$ from a reduced number, P/L, of projections. This reduction process is performed by shifting the truncated projections, $\hat{\mathcal{K}}_M[\vec{\delta}]g(\theta_p, t)$ of f', by $\tau(\theta, \vec{\delta})$ in t (see Fig. 1), decimating the P projections in angle into P/L projections, and shifting back in t by $-\tau(\theta, \vec{\delta})$.

Using $\mathcal{O}[L, M, \delta]$ to denote the projection reduction operator, the exact formula (2) for backprojection onto subimage f' is replaced by the approximation

$$f' = \mathcal{K}_M[\vec{\delta}]f = \mathcal{B}_{M,P/L}[\vec{\delta}]g' \tag{5}$$

$$= \mathcal{B}_{M,P/L}[\vec{\delta}]\mathcal{O}[L, M, \vec{\delta}]g, \tag{6}$$

where $\mathcal{B}_{M,P/L}$ is a backprojection onto an $M \times M$ subimage using P/L projections. This leads to an approximate decomposition of the backprojection operation for a partitioned image that is analogous to (4),

$$f = \mathcal{B}_{N,P}[\vec{0}]g = \sum_{j=1}^{4} \mathcal{B}_{N/2,P/2}[\vec{\delta}_j]\mathcal{O}[2, N/2, \vec{\delta}_j]g. \tag{7}$$

This decomposition is illustrated in Fig. 2.

The decomposition (7) is applied recursively, at each level further partitioning the subimages into smaller subimages in accordance with (3). The recursion can be continued until the subimages are of some desired minimum size $M_{\min}$, and then the backprojections $\mathcal{B}_{P_{\min},M_{\min}}$ performed. The optimum $M_{\min}$ is usually implementation-dependent. It can be chosen as small as $M_{\min} = 1$, so that the smallest subimages are 1 pixel in size. In this case there will be $\log_2 N$ decomposition levels. The last level will involve N^2 single pixel backprojections $\mathcal{B}_{P/N,1}$, with a total cost of cPN. Assuming fixed length interpolators are used for the decimation and shift operations in the implementation of $\mathcal{O}[2, M, \vec{\delta}_j]$, it can be shown that the computational cost of each level will be

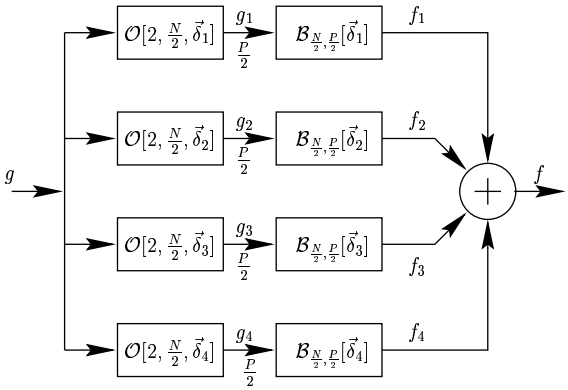

Fig. 2. Approximate decomposition of the fan-beam backprojection, with reduction of number of projections.

$c_1 NP$. The total cost of the $\log_2 N$ levels is therefore $O(PN \log N)$, and because $P = O(N)$, the total cost of the recursive decomposition algorithm becomes $O(N^2 \log N)$.

The implementation of the recursive decomposition is simplified by the following observation. The operations of projection shift in t and projection truncation commute (with appropriate coordinate transformations). Therefore, the shift operation of one stage, can be combined with that of the following stage. Likewise, the shift operation occurring just before the final subimage backprojection $\mathcal{B}_{M_{\min},P_{\min}}$ can be combined with the interpolation operations in the backprojection itself. Thus, in a recursive implementation, $\mathcal{O}[L, M, \vec{\delta}_j]$ requires only one projection shift step per stage.

In practice, projection data are acquired by discrete detectors and therefore sampled in t with interval T. Because the filtered projections are bandlimited in t, the required projection shifts by noninteger multiples of T can be accomplished using a combination of interpolation and resampling [4]. Importantly, with the specific projection shifting scheme proposed here, the sampling interval of the projections remains uniform and constant, so that the interpolation and resampling can be efficiently implemented by simple digital filters. Because the fractional shifting error decays exponentially with the length of the filter, short filters – even simple linear interpolation – usually suffice. The t-interpolation accuracy also increases by oversampling the projections in t, which, if desired, can be performed efficiently by digital interpolation of the projections.

The accuracy of the backprojection obtained using the approximate decomposition can be increased by angular oversampling, that is increasing the ratio $(P/L)/M$ between the number of projections used in the backprojections, and the size of the subimages. This can be achieved by using exact decompositions, which decrease the size of the subimages without reducing the number of projections. The recursive decomposition usually includes such exact decomposition steps, whose number Q provides yet another method to control the tradeoff between accuracy and computation.

In summary, an important distinction between the hierarchical fan-beam algorithm and the parallel-beam FHBP of [4], is that no shifting and recentering of subimages takes place; instead, only projections are shifted. All subimage backprojection operations are performed in absolute image coordinates, to preserve the correct weighting in (1), which depends on these coordinates. The

same principles allow to extend the algorithm to 3D cone-beam backprojection for various scanning geometries.

4. SIMULATION RESULTS

We used the so-called unmodified Shepp-Logan head phantom of size $N \times N = 512 \times 512$ phantom, with a realistic (and high) contrast between the skull and brain. This presents a challenging test for the algorithm, because even slight artifacts created by the reconstruction of the skull are prominent on the brain background.

We set the source-to-image-center distance to 1.25 times the image size,i.e., $D = 1.25N$, and the total fan angle to $2\alpha_0 = 1.17$ radians, with 1025 detectors on the fan. We generated full-scan fan-beam projection data with $P = 1024$ evenly spaced source angles, $\theta_p \in [0, 2\pi]$ for the 10-ellipse phantom, using analytical expressions for the line integrals through an ellipse [1].

Figure 3 compares the exact backprojection algorithm and our fast fan-beam backprojection algorithm. The speedups of the fast algorithms are $\times 30$ and $\times 60$ for $Q = 1$ and $Q = 2$ exact decompositions in the recursion, respectively. The reconstructions using the conventional exact and the fast backprojection algorithms show little if any perceptual quality difference at either operating point. The point-spread-functions (not shown) for the exact and fast algorithm are virtually identical.

5. REFERENCES

[1] A. C. Kak and M. Slaney, *Principles of Computerized Tomographic Imaging*. New York, NY: IEEE Press, Inc., 1988.

[2] W.A. Kalender, *Computed Tomography: Fundamentals, System Technology, Image Quality, Applications*, Munich: Publicis MCD Verlag, 2000.

[3] F. Natterer and F. Wübbeling, *Mathematical Methods in Image Reconstruction*. Philadelphia: SIAM, 2001.

[4] S. Basu and Y. Bresler, "An $O(N^2 \log N)$ filtered backprojection reconstruction algorithm for tomography," *IEEE Trans. Image Processing*, vol. 9, pp. 1760–1773, Oct. 2000.

[5] S. Nilsson, *Application of fast backprojection techniques for some inverse problems of integral geometry.* Ph.D. thesis, Department of Mathematics, Linköping University, 1997.

[6] P.-E. Danielsson, "Iterative techniques for projection and back-projection," Tech. Rep. LiTH-ISY-R-1960, ISSN 1400-3902, Department of Electrical Engineering, Linköping universitet, 1997.

[7] M. Ingerhed, *Fast backprojection for computed tomography, implementation and evaluation*. Tech. Rep. Liu-TEK-LIC-1999:17 , Department of Electrical Engineering, Linköping universitet, Sweden 1999.

[8] A. Brandt, J. Mann, M. Brodski, and M. Galun, "A fast and accurate multilevel inversion of the Radon transform." *SIAM J. Appl. Math.*, vol. 60, no. 2, pp. 437-462, 1999.

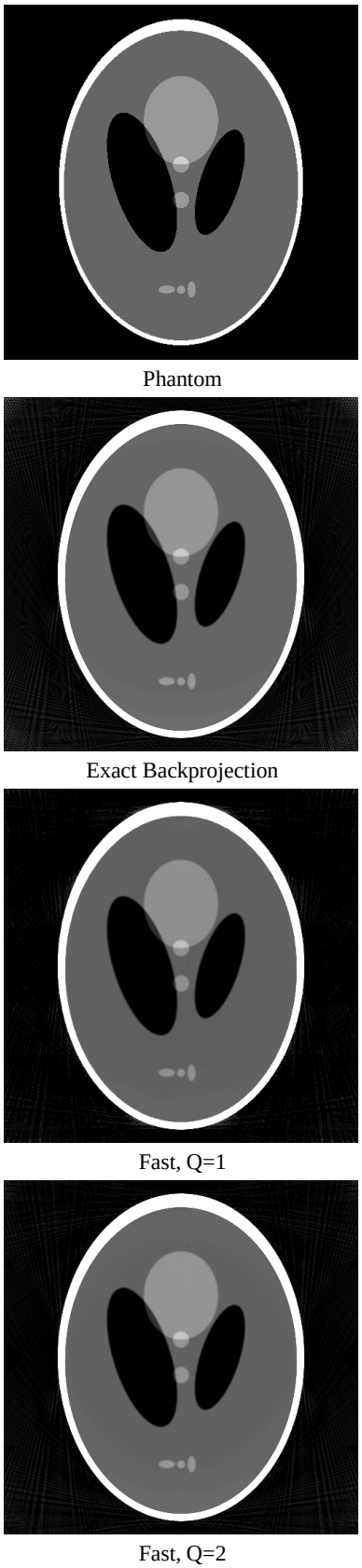

Fig. 3. Comparison of exact and fast fan-beam backprojections for colinear equispaced detectors.